Comparative analysis of the microstructure and mechanical properties of an Al-Cu-Mg-Ag alloy peak-aged at relatively low and high temperatures

IOP Conf. Series: Materials Science and Engineering **672** (2019) 012027 doi:10.1088/1757-899X/672/1/012027

Comparative analysis of the microstructure and mechanical properties of an Al-Cu-Mg-Ag alloy peak-aged at relatively low and high temperatures

M Gazizov[1], R Holmestad[2] and R Kaibyshev[1]

[1] Belgorod State University, Pobeda 85, Belgorod, Russia
[2] Department of Physics, Norwegian University of Science and Technology (NTNU), Trondheim, Norway

E-mail: gazizov@bsu.edu.ru

Abstract. The mechanical properties and microstructure have been investigated in the Al-4.35Cu-0.46Mg-0.63Ag-0.36Mn-0.12Ti-0.04Fe alloy (in wt. %) peak-aged at 150 °C and 190 °C. The yield stresses (YS) and the ultimate tensile strength (UTS) were insignificantly higher by 15 MPa and 5 MPa, respectively, after peak-aging at 150 °C for 24 h compared with 190 °C for 1.5 h. Elongation-to-failure (δ) was the same (~6%) in both states. Microstructure analysis showed great differences in the morphology of precipitates within grain/subgrain interiors, as well as in the structure of regions adjacent to grain boundaries (GBs). Relationships between strength/ductile properties and microstructure were discussed.

1. Introduction

Al-Cu-Mg-Ag alloys exhibit high specific strength, good fracture toughness and resistance to fatigue fracture, as well as superior creep resistance. This attractive combination of mechanical properties is attributed to the Ω-phase precipitated during aging as uniformly distributed plates along the $\{111\}_{Al}$ planes [1–5]. The Ω-phase has a sandwich-like structure composed from a core having a nominal composition and a crystal structure similar to the equilibrium θ-phase (*I4/mcm*) observed in Al-Cu alloys [1,2,6]. Furthermore, the transition ordered layers of Mg and Ag provide a coherent structure of broad interfacial boundaries and relatively high resistance to coarsening of the plates at elevated temperatures [1–4,7]. It has been shown [3] that disperse $\{111\}_{Al}$ plates are highly efficient in strengthening aluminum alloys compared with spherical particles or other rationally oriented precipitates, such as $<100>_{Al}$ rods and $\{100\}_{Al}$ plates. One of the simplest ways to additionally enhance the strength of an age-hardenable aluminium alloy is to optimize the aging temperature, which leads to the increased contribution of the precipitate strengthening to the overall strength of the material. This aim can be reached by the formation of finer precipitates of metastable phases and/or an increase in its volume fraction occurring in accordance with thermodynamics at lower aging temperatures [2,6]. Regarding the Ω-phase, the relationships between the strength properties and morphology of the $\{111\}_{Al}$ plates of this phase at relatively low temperatures in Al-Cu-Mg-Ag alloys, have not been well studied. Thus, the aim of the present work is to characterize the precipitate microstructure in relationship with the peak mechanical properties of an Al-Cu-Mg-Ag alloy reached after aging at relatively low (150 °C) and high (190 °C) temperatures.

2. Experimental procedure

An aluminum alloy with the chemical composition Al-4.5Cu-0.56Mg-0.77Ag-0.42Mn-0.12Ti-0.05V-0.02Fe (in wt. %) was prepared using a direct-chill semi-continuous casting process. The alloy was homogenized at 500 °C for 24 h, followed by cooling in a furnace, then it was extruded at ~400 °C with a ratio of ~2.6 and subjected to hot rolling with a reduction of ~60%. The resulting 20 mm thick plates were used to cut rectangular samples with a size of ~20×20×3 mm and flat "dog-bone" samples with gauge sizes of 35×7×3 mm using a wire electric discharge machine. The samples were solution heat treated at 510 °C for 1 hour, followed by water-quenching and immediately aged at 150 °C and 190 °C at different times (up to 200 h).

Hardness was measured in arbitrarily selected areas of the flat surface of rectangular samples using a Wilson Wolpert 402 MVD hardness tester at a constant load of 5 N and a loading time of 15 s. Tensile properties (YS, UTS and δ) were measured using an Instron 5882 tensile testing machine at an initial strain rate of ~10^{-3} s^{-1}. At least ten hardness indentations and three tensile tests were carried out for each condition to determine the standard deviation and the average tensile properties, respectively.

The methodology for preparing TEM foils was described in [3]. TEM characterization was performed using a JEOL JEM-2100F microscope operating at 200 kV. Precipitate parameters (diameter, thickness, number density and volume fraction) were analyzed in accordance with [3,4].

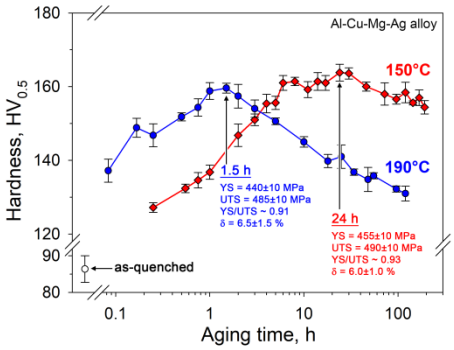

Figure 1. Hardness evolution during aging at 150 °C and 190 °C.

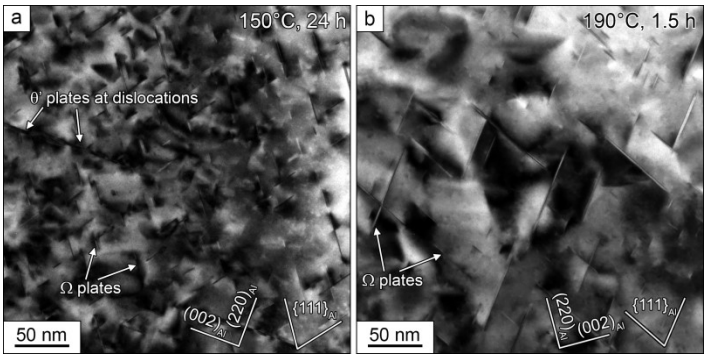

Figure 2. Microstructure of the alloy at peak-aging conditions after aging at 150 °C (a) and 190 °C (b).

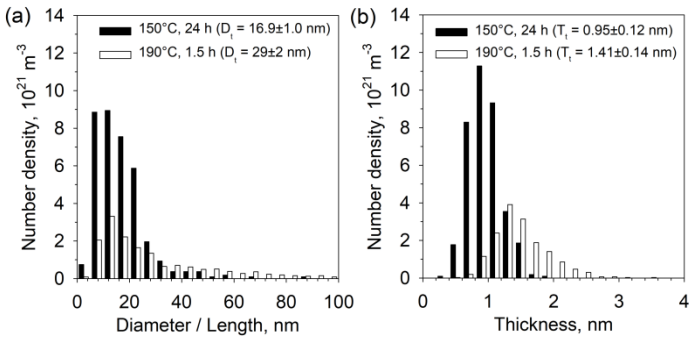

Figure 3. Effect of aging on the distribution of the Ω-plate diameters (a) and thicknesses (b) within the grains.

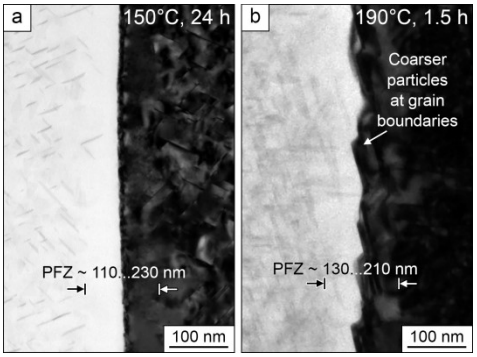

Figure 4. PFZs adjacent to the GBs after aging at 150°C (a) and 190°C (b).

3. Results and discussions

3.1. Mechanical properties

Figure 1 shows the hardness evolution as a function of the aging time at 150 °C and 190 °C. It is seen that the three stages (under-, peak- and over-aging) being consistent with thermodynamics at different

aging temperatures [1,2,6] can be identified at both aging temperatures. The hardness was ~86 $HV_{0.5}$ in the as-quenched state. At the initial aging stage, the hardness increased dramatically with prolonged aging. Peak hardness values of ~160 $HV_{0.5}$ and ~165 $HV_{0.5}$ were obtained in the range of 1-2 h at 190 °C and 14-30 h at 150 °C, respectively. The results of the analysis of tensile properties are put into figure 1. During further aging, the hardness decreased slowly, but preserved a relatively high level during aging at 150 °C even after ~200 h compared with aging at 190 °C, where the decrease in hardness was much more pronounced. This can indicate that the precipitation kinetics was much higher at 190 °C than at 150 °C, but the relatively close maximum strength indicates a small difference in precipitate morphology obtained in peak hardness for both temperatures [1,2,6]. Samples after 150 °C and 190 °C for 1.5 h and 24 h, respectively, were chosen for the TEM characterization.

Table 1. The Ω precipitate parameters within the grains/subgrains in peak-aging stage.

Aging	N_V, 10^{21} m^{-3}	F_V, %	Aging	N_V, 10^{21} m^{-3}	F_V, %
150°C, 24 h	36.4±1.3	0.8±0.3	**190°C, 1.5 h**	15.9±1.8	1.5±0.3

3.2. Microstructure

The initial microstructure of the alloy in the as-quenched state (not shown) consists of elongated grains/subgrains having average sizes of ~27 and ~17 μm in the longitudinal and transverse directions, respectively. Uniformly distributed dispersoids were observed in the matrix. The average diameter size and volume fraction of them were ~50 nm and 0.5%, respectively.

Representative TEM images showing precipitate microstructures at the peak hardness stages, are given in figure 2. Particles in the form of platelets with the $\{111\}_{Al}$ habit planes were identified as Ω-phases. The Ω-phase plates nucleated homogeneously in the grain/subgrain interiors. The distributions of the apparent diameters and thicknesses of the $\{111\}_{Al}$ plates (in figures 3a and b, respectively) show that the size of the Ω-phase is different in the two states. It seems that a bimodal distribution of the plate diameters takes place after peak-aging at 190 °C. As a result, the diameter distribution peak is narrower at 150 °C compared with aging at 190 °C, where a competitive growth of relatively long and short Ω plates is observed. It should be noted that, firstly, for the short and long plates at 190 °C there is no obvious difference in thickness between them, but they are thicker at 190 °C than at 150 °C; secondly, the diameters of the short ones at 190 °C can be commensurable with the diameters of the Ω plates at 150 °C. Number density (N_V) and volume fraction (F_V) of the $\{111\}_{Al}$ plates have also been estimated (table 1). It is seen that the low temperature aging provides the formation of smaller Ω plates having a higher number density but lower volume fraction compared with aging at 190 °C. The precipitation strengthening contribution to the overall strength of the alloy due to shearing the $\{111\}_{Al}$ plates has been roughly estimated using equations from work [3] and an interfacial energy of 0.165 $J \times m^{-2}$ equal to ~214 MPa and ~225 MPa after aging at 150 °C and 190 °C, respectively.

A TEM analysis of structures of the GBs has been performed due to their importance for the mechanical behavior of the aged aluminum alloys [8]. Examples of TEM images of the alloy in peak-aging states at 150 °C and 190 °C are shown in figure 4. The widths of the precipitate free zones (PFZ) adjacent to GBs were measured to be in a similar range in both states. This is inconsistent with the hypothesis of precipitation in the age-hardenable alloys – wider PFZs can be formed at higher aging temperatures due to the lower driving force for precipitation and the higher critical supersaturation of vacancies needed for nucleation to occur, in comparison with low temperatures [2,6]. It has also been shown [5,7] that Mg-Ag clusters play an important role in the heterogeneous mechanism of nucleation of the Ω-phase. It seems that the effect of the vacancy concentration on this type of cluster formation is less pronounced at the studied aging temperatures. Further, the most obvious difference in the studied peak-aged alloys was in the particle dispersion at the GBs. The PFZ widths varied in the same range for 150 °C and 190 °C, meanwhile coarser particles with a higher volume fraction were observed along the GBs at 190 °C. This is inconsistent with the amount of solute elements, which are available for precipitation close to the GBs, and is probably the result of a more complicated diffusion

process. For the age-hardenable Al alloys, the narrower PFZ and fine precipitations on the GBs are favorable for the plasticity of these alloys. For this reason, the regions adjacent to the GBs occupied by coarser particles should exhibit a lower plasticity in the alloy aged at 190 °C compared with 150 °C. However, the δ values (figure 1) are the same after aging at both temperatures. For this reason, the two factors contrary affecting the plasticity can act together. An example of the latter one can be grain/subgrain interiors, demonstrating higher plasticity due to the different precipitate microstructure [1,2].

Precipitates elongated along the $<001>_{Al}$ directions in the $\{110\}_{Al}$ projection were identified as plates of the θ'-phase. At both aging temperatures, the θ' plates were non-uniformly distributed in the matrix. They can be found as nucleated along dislocation lines. It should be noted that the fraction of the θ'-phase was lower at 190 °C compared with aging at 150 °C, where its number density was less than 5% of the total number density of all precipitates ($\{111\}_{Al}$ and $\{001\}_{Al}$ plates) found. Thus, the Ω-phase plates are the main strengthening phase because of their dominant fraction compared to other secondary precipitates, such as the θ′-phase, as well as dispersoids in the alloy after 150 °C and 190 °C peak-aging. Thus, aging at 150 °C and 190 °C provides a large difference in the precipitate morphology, meanwhile similar strength and ductile properties were obtained. To better understand this phenomenon, further comprehensive investigations are required.

4. Conclusions

The microstructure and precipitation in relationship with the mechanical properties were analyzed in the Al-4.35Cu-0.46Mg-0.63Ag-0.36Mn-0.12Ti-0.04Fe (wt. %) alloy aged at 150 °C for 24 h and 190 °C for 1.5 h. Small differences in the tensile strength properties were observed. Analysis of the precipitate strengthening contributions showed that similar increments to the overall strength of the alloy took place despite a significant difference between the precipitate morphology in the grain/subgrain interiors after aging at 150 °C and 190 °C. PFZ widths varied in similar ranges in both states, but coarser particles at the GBs were found at 190 °C. Ductility attributed to the plastic grain interiors and PFZ, expecting to show a less plastic or even brittle fracture mode after aging at 190 °C, were similar to the samples aged at 150 °C, where finer particles appear at the GBs.

Acknowledgments

This work is financially supported by Council for Grants of the President of the Russian Federation (No. 075-02-2018-164**)** and the Faculty of Natural Sciences at NTNU, Norway (Project No. 81617879). The TEM work was carried out on the NORTEM infrastructure (Grant 197405) at NTNU. The authors are grateful to the staff of the TEM Gemini Center at NTNU and the Joint Research Center at BelSU for their assistance with the structural and mechanical characterizations.

References

[1] Polmear I J 2006 *Light alloys: from Traditional Alloys to Nanocrystals* (Oxford: Butterworth-Heinemann/Elsevier)
[2] Nie J F 2014 Physical Metallurgy of Light Alloys *Physical Metallurgy: Fifth Edition* vol 3 (Elsevier) pp 2009–156
[3] Gazizov M and Kaibyshev R 2017 *Mater. Sci. Eng.* A **702** 29
[4] Gazizov M and Kaibyshev R 2017 *Mater. Sci. Technol.* **33** 688
[5] Gazizov M and Kaibyshev R 2015 *Mater. Sci. Eng.* A **625** 119
[6] Porter D A, Easterling K E and Sherif M Y 2014 *Phase Transformations in Metals and Alloys* (New York: CRC press)
[7] Bai S, Liu Z, Zhou X, Xia P and Zeng S 2014 *J. Alloys Compd.* **602** 193
[8] Christiansen E, Marioara C D, Marthinsen K, Hopperstad O S and Holmestad R 2018 *Mater. Charact.* **144** 522